

G. Turlybay , E. Nurgaziyeva , D. Issayeva ,  
A. Mentbayeva , Z. Bakenov , S. Kalybekkyzy\* 

<sup>1</sup>National Laboratory Astana, Astana, Kazakhstan

<sup>2</sup>School of Engineering and Digital Sciences, Nazarbayev University, Astana, Kazakhstan

<sup>3</sup>School of Sciences and Humanities,

Nazarbayev University, Astana, Kazakhstan

\*e-mail: sandugash.kalybekkyzy@nu.edu.kz

(Received 19 October 2023; received in revised form 15 November 2023; accepted 03 December 2023)

## Synthesis and characterization of LATP solid electrolyte by solution method

**Abstract.** Recently, considerable attention has been paid to the study of solid electrolytes in lithium-ion batteries. Ion conductive ceramic material NASICON-type  $\text{Li}_{1+x}\text{Al}_x\text{Ti}_{2-x}(\text{PO}_4)_3$  (LATP) is a promising solid electrolyte for lithium-ion batteries due to its stability in air. In this work successfully produced pure solid electrolyte LATP powders with a rhombohedral NASICON-type structure. Here we report the results of LATP synthesis using the solution method. Pellets of dense electrolyte were made at 900 °C. It has been found that the ionic conductivity of LATP is largely influenced by the preparation method. Pure LATP was obtained with the grain size of 100-700 nm. These findings demonstrate the efficacy of the solution method in producing pure LATP. The resultant LATP has an activation energy of 0.465 eV and a total lithium-ion conductivity of  $5.8 \times 10^{-5}$  S cm<sup>-1</sup> at ambient temperature. Its typical particle size is between 100 and 700 nm, and its relative density is 89.5 percent.

**Key words:** solid electrolytes, LATP, ionic conductivity, NASICON type, X-ray diffraction, SEM.

### Introduction

In the last twenty years, the lithium-ion battery (LIBs) has gained popularity as a preferred option for rechargeable batteries because of its low redox potential, high energy density, minimal self-discharge, and lack of a memory effect. Currently, LIBs are extensively used in energy storage applications like 5G mobile networks, electric vehicles, and large-scale grid energy due to their lightweight and high energy density. LIBs incorporating organic liquid electrolytes face issues related to leakage and flammability, posing significant constraints, especially in the context of large-scale applications. These challenges not only compromise the safety of LIBs but also hinder their widespread implementation on a larger scale. However, the use of flammable organic liquid electrolytes in LIBs poses safety concerns, limiting their practical applications [1, 2, 4, 5]. The emergence of all-solid-state lithium-ion batteries (ASSLIBs), incorporating solid-state electrolytes (SSEs), is driven by the objective to improve safety without compromising the advantages of conventional LIBs. However, the practical application of ASSLIBs is

hindered by the suboptimal ionic conductivity of these solid-state electrolytes. Consequently, there is a need for enhancements in both ionic conductivity and the mechanical and electrochemical stability of SSEs to unlock the full potential of ASSLIBs.

During battery operation, anions and cations move between electrodes, but anions, not participating in the oxidation-reduction reaction, cause concentration polarization on both sides of the electrolyte. This leads to rapid lithium dendrite growth, potentially penetrating the membrane and causing a short circuit, posing a safety risk [14].

Concerns over the frequent safety issues associated with traditional batteries have prompted a shift towards all-solid-state batteries. In addressing this, solid electrolytes are being employed to replace liquid electrolytes in the all-solid-state lithium-ion battery (ASSLIBs) system [11, 14]. This adaptation aims to eliminate electrolyte leakage, curb the growth of lithium dendrites, and elevate overall battery safety. The solid-state electrolyte holds a pivotal position in ASSLIBs, contributing significantly to advancements in carbon economy and energy technologies [12, 14].

Inorganic-based electrolytes typically exhibit high ion conductivity. Various solid inorganic materials show promise for application in lithium-ion batteries. Presently, advanced solid electrolytes, including lithium halide, lithium hydride perovskite, lithium nitride, garnet, argyrodite, and sulfide, demonstrate ionic conductivity within the range of  $10^{-6}$ – $10^{-2}$  S  $\text{cm}^{-1}$ . These materials hold potential for enhancing the performance of lithium-ion batteries through improved conductivity characteristics [3,4]. The sulfide type of electrolyte has the highest ionic conductivity among all other types of solid electrolytes, which is close to a liquid electrolyte ( $10^{-2}$  S  $\text{cm}^{-1}$ ). However, it is unstable in air which prevents its mass production.

Among all types of solid electrolytes, NASICON structured electrolytes are the most stable in air and have sufficient ionic conductivity in the range of  $10^{-6}$ – $10^{-3}$  S  $\text{cm}^{-1}$  [1–13]. The NASICON-type electrolyte with the general formula of  $\text{NaM}_2(\text{PO}_4)_3$  has a rhombohedral structure with the space group R3c. Na atoms can be replaced with Li atoms by converting them to  $\text{LiM}_2(\text{PO}_4)_3$ , where M is Ti, Zr or Ge [2]. The titanium-containing type is  $\text{LiTi}_2(\text{PO}_4)_3$  (LTP), which demonstrates high chemical and thermal stability with an applicable ionic conductivity of  $10^{-4}$  S  $\text{cm}^{-1}$  in grains and a total conductivity of about  $10^{-8}$  and  $10^{-6}$  S  $\text{cm}^{-1}$  due to high resistance at grain boundaries [10].

Various types of inorganic solid-state electrolytes, including garnet-type  $\text{Li}_7\text{La}_3\text{Zr}_2\text{O}_{12}$  [3], perovskite-type  $\text{Li}_x\text{La}_{2/3-x}\text{TiO}_3$  [5,6], and NASICON-type systems [12,13], are currently under active investigation. Among these, the NASICON-type material lithium titanium phosphate,  $\text{LiTi}_2(\text{PO}_4)_3$  (LTP), stands out as a particularly promising solid-state electrolyte due to its intrinsic safety features, cost-effectiveness, and high thermal and air stability at room temperature. LTP has demonstrated versatility, serving not only as an effective electrolyte in ASSLBs [4] but also in lithium-air and lithium-sulfide systems [2].

The  $\text{LiTi}_2(\text{PO}_4)_3$  material, belonging to the NASICON type, adopts a rhombohedral structure characterized by octahedral  $\text{TiO}_6$  units that share corners with tetrahedral  $\text{PO}_4$  units. Within this structure, two types of Location vacancies are present: M1 vacancies, situated between tetrahedral  $\text{PO}_4$  units, and M2 vacancies, formed between adjacent octahedral  $\text{TiO}_6$  units. In the 3D NASICON network, the diffusion of  $\text{Li}^+$  ions occurs along pathways that connect the M1–M2 vacancies. This intricate structure facilitates the movement of lithium ions within the material [15].

However,  $\text{LiTi}_2(\text{PO}_4)_3$  suffers from a drawback of lower ionic conductivity at room temperature [14]. In the case of LTP, the grain boundary resistance significantly outweighs the contribution of the bulk to the total resistance. This indicates that the grain boundary resistance plays a pivotal role in governing the overall conductivity of  $\text{LiTi}_2(\text{PO}_4)_3$ . Therefore, the optimization of total conductivity crucially depends on controlling the density of an LTP electrolyte. To enhance density, researchers have explored the effects of incorporating fluxes or employing novel sintering techniques, some of which are briefly discussed below [15].

Studies show that  $\text{Ti}^{4+}$  can be replaced by various trivalent elements (such as  $\text{Al}^{3+}$ ,  $\text{Fe}^{3+}$ ,  $\text{Y}^{3+}$ ,  $\text{Cr}^{3+}$ ,  $\text{Ga}^{3+}$ , and  $\text{Sc}^{3+}$ ) while preserving the rhombohedral NASICON-type structure [12–14]. Among these aliovalent substituents,  $\text{Al}^{3+}$  has proven effective in adjusting the NASICON cell volume to an optimal size for facilitating  $\text{Li}^+$  transport, significantly improving conductivity in resulting  $\text{Li}_{1-x}\text{Al}_x\text{Ti}_{2-x}(\text{PO}_4)_3$  (LATP). Conversely, some research highlights that the aluminum additive primarily forms the Al-rich second phase  $\text{AlPO}_4$ , enhancing total ion conductivity by promoting densification and effectively creating a composite. However, the concentration of added Al is crucial, as at high levels, it hinders Li-ion conduction across the  $\text{LiTi}_2(\text{PO}_4)_3$  grain boundaries. Therefore, maintaining overall control of the LTP microstructure is vital to maximize overall conductivity, striking a balance between achieving high density and ensuring that secondary phases do not impede ionic transport at the grain boundaries [15].

To address the microstructure challenge, an alternative approach involves utilizing low melting point fluxes to enhance the density of  $\text{LiTi}_2(\text{PO}_4)_3$  (LTP) and related substituted solid electrolytes.

Currently, there are several known methods for the preparation of lithium aluminum titanium phosphate (LATP) samples. These include solid-phase reaction, sol-gel method, coprecipitation method, and melt quenching, as well as advanced techniques like spray drying, spark plasma sintering, and hydrothermal synthesis. These diverse methods offer researchers a range of options for tailoring LATP samples to specific requirements in terms of structure, composition, and performance [2,3,7,9].

Within these methods, the solid-phase reaction method encounters challenges related to the formation of secondary phases. Additionally, the melt quenching process demands elevated sintering temperatures. As a result, these factors need to be carefully considered and addressed to optimize the efficiency of the synthesis process [11]. The coprecipitation method

involve in the complexing agent or co precipitator, which results in higher production cost. Therefore, it is meaningful to explore a low-cost method for the preparation of LAMP samples.

A sol-gel technique, specifically the solution method, stands out as a straightforward and cost-effective approach. This low-temperature process involves dissolving all precursors to form a homogeneous phase, facilitating the production of nanomaterials characterized by high crystallinity in a pure state. The simplicity and affordability of this method make it an attractive option for synthesizing materials with desired properties [1, 10].

The primary objective of this study is to acquire nanoparticles of lithium aluminum titanium phosphate (LAMP) with a focus on solid electrolytes. In this research, we explore a straightforward solution method tailored for the large-scale production of nanoscale LAMP ( $x=0.3$ ). This method, utilizing purified water as a solvent, aims to circumvent the hydrolysis of titanium salt and achieve enhanced ionic conductivity. Furthermore, this work introduces a novel strategy for the synthesis of additional LAMP solid electrolytes with varying  $x$  values, expanding the applicability of the proposed approach.

## Materials and methods

*Preparation of solid electrolyte.* The preparation of  $\text{Li}_{1.3}\text{Al}_{0.3}\text{Ti}_{1.7}(\text{PO}_4)_3$  solid electrolyte involved a solution-based method. Initially,  $\text{LiOH}\cdot\text{H}_2\text{O}$  was dissolved in purified water. Subsequently,  $\text{Al}_2\text{O}_3$ ,  $\text{TiO}_2$  and  $\text{H}_3\text{PO}_4$  were introduced into the solution under magnetic stirring. The resulting mixture underwent drying at  $180\text{ }^\circ\text{C}$  in an oven to eliminate excess water, leading to the formation of a viscous paste. This paste was subjected to calcination at  $700\text{ }^\circ\text{C}$  for 6 hours. The resultant precursor powders were then subjected to high-energy mechanical ball grinding, utilizing zirconium balls with a 12 mm diameter, at 650 rpm for 5 hours. The ground powders were subsequently pressed into pellets with a hydraulic press, featuring a diameter of 10 mm. These pellets underwent sintering at  $900\text{ }^\circ\text{C}$  for 12 hours in an air environment to yield the final LAMP pellets.

This methodological approach ensures the systematic synthesis of  $\text{Li}_{1.3}\text{Al}_{0.3}\text{Ti}_{1.7}(\text{PO}_4)_3$  solid electrolyte, employing a well-defined sequence of steps to achieve the desired material properties.

*Characterization.* The structure of LAMP before and after sintering was studied using XRD (Rigaku smartLAB X-ray system) equipped with a Cu X-ray tube and a D-Text detector within  $2\theta = 10\text{-}70^\circ$  with a step width of  $0.06^\circ$ .

The grain size and morphology of the LAMP powder and pellet were studied using SEM (FESEM Auriga, Crossbeam 540). Gold with a thickness of 5 nm was applied to the surface of the powders using an automatic Q150T atomizer to improve electronic conductivity, since the electrolyte materials are electronic insulators. Ionic conductivity was measured by electrochemical impedance spectroscopy (potentiostat/galvanostat, Metrohm AutoLab 204, 1 Hz – 1 MHz).

## Results and discussion

The solution method has proven effective in the successful synthesis of pure NASICON-structured lithium aluminum titanium phosphate (LAMP). The X-ray diffraction (XRD) pattern, as depicted in Figure 1, reveals that the predominant phase is NASICON, characterized by the spatial group R3c. Notably, a common challenge in LAMP material preparation lies in the significant formation of  $\text{AlPO}_4$ . In Figure 1, the arrow in the powder form points to the peak corresponding to  $\text{AlPO}_4$ . This undesirable phase typically arises during high-temperature sintering, leading to the loss of lithium through evaporation [13]. However, in the case of the obtained pellet powder, the intensity of the  $\text{AlPO}_4$  peak decreases, indicating a reduction in the amount of  $\text{AlPO}_4$ . The lattice constants, calculated from the XRD data, are measured at 0.8471 nm and 2.0763 nm, aligning with the spatial group R3c.

These findings underscore the efficacy of the solution method in achieving the desired NASICON structure for LAMP, while also addressing the challenge of minimizing the formation of  $\text{AlPO}_4$  during the synthesis process. The reduced presence of  $\text{AlPO}_4$  in the pellet powder indicates progress in optimizing the material composition and characteristics.

SEM images were acquired to analyze the morphology of the synthesized ATP. As per existing literature [2], the particles are expected to exhibit a cubic shape with dimensions ranging from 1 to 2 microns. Figure 2a reveals that LAMP particles, obtained through the solution method, exhibit a reduced size in the range of 100-700 nm. This diminution in particle size is highly favorable, as it results in a smaller surface area, thereby minimizing the impact of grain boundaries on the overall conductivity of lithium ions [1-2].

Figure 2b provides a visualization of the surface morphology of the LAMP pellets, offering valuable insights into the structural characteristics of the synthesized material.

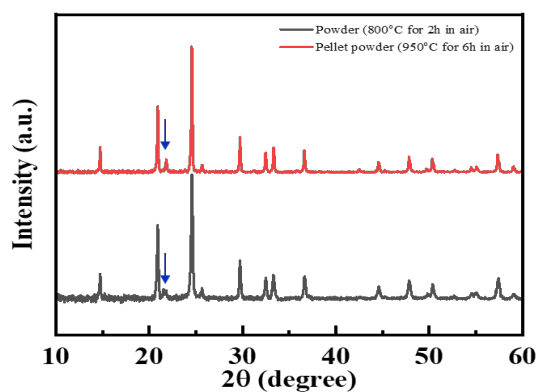


Figure 1 – XRD images of the prepared LATP in the form of powder and pellet

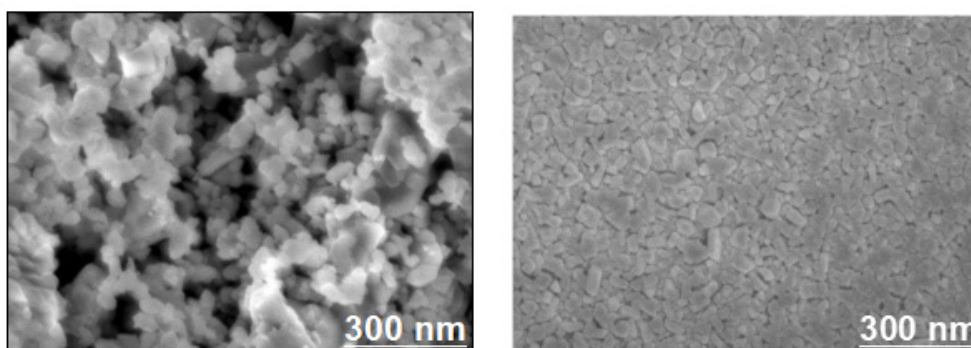


Figure 2 – SEM images of: a) LATP powder b) LATP pellet

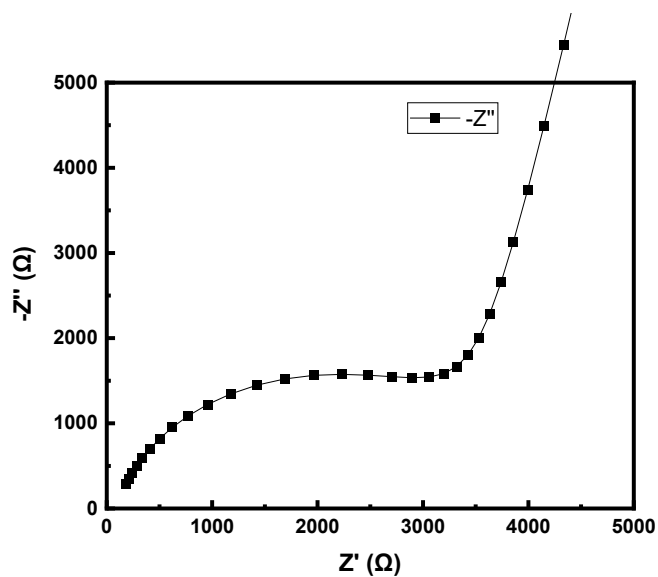


Figure 3 – Impedance profile measured at room temperature for LATP pellet

According to the impedance spectrum (Figure 3), measured ionic conductivity of the above-obtained LATP pellet was  $5.8 \times 10^{-5}$  S cm<sup>-1</sup>. The low ionic conductivity might be due to the density and activation energy of Li<sup>+</sup> transport. The ionic conductivity of LATP is directly proportional to its

density in pellet form [5]. The calculated density of the obtained LATP pellet is 89.7 % (Table 1). This value is probably not enough to achieve ionic conductivity above  $5.8 \times 10^{-5}$  S cm<sup>-1</sup>. Furthermore, calculated activation energy for Li<sup>+</sup> transport in LATP pellet is 0.465 eV.

**Table 1** – Pellet parameters

Parameters	Density, %	Ionic conductivity, S cm <sup>-1</sup>	Activation energy, eV
Indicators	89.7	$5.8 \times 10^{-5}$	0.465

## Conclusion

In this work, pure solid electrolyte LATP powders with a rhombohedral NASICON-type structure were successfully obtained. Dense electrolyte pellets were prepared at 900 °C. These results show that the solution method is an effective approach for obtaining pure LATP. The resulting LATP with an average particle size of 100-700 nm and a relative density of 89.7 % demonstrates a total lithium-ion conductivity of  $5.8 \times 10^{-5}$  S cm<sup>-1</sup> at room temperature and an activation energy of 0.465 eV. Based on the achieved parameters prepared LATP is a promising solid electrolyte for all solid-state lithium-ion batteries.

## Acknowledgement

This research was supported by the research grant #AP14871520 “Synthesis of ultra thin composite polymer electrolytes with enhanced characteristics for Li-ion batteries” from the Ministry of Science and Higher Education of the Republic of Kazakhstan

## References

1. Kotobuki M., Koishi M. (2013) Preparation of Li<sub>1.5</sub>Al<sub>0.5</sub>Ti<sub>1.5</sub>(PO<sub>4</sub>)<sub>3</sub> solid electrolyte via a sol-gel route using various Al sources. *Ceramics International*, vol. 39, no. 4, pp. 4645-4649, <https://doi.org/10.1016/j.ceramint.2012.10.206>.
2. Xiao W., Wang J., Fan L., Zhang J., Xifei Li. (2019) Recent advances in Li<sub>1+x</sub>Al<sub>x</sub>Ti<sub>2-x</sub>(PO<sub>4</sub>)<sub>3</sub> solid-state electrolyte for safe lithium batteries, *Energy Storage Materials*, vol. 19, pp. 379-400, <https://doi.org/10.1016/j.ensm.2018.10.012>.
3. Zhang, H., Wu, X., Yang, T., Liang, S., Yang, X. (2013). Cooperation behavior between heterogeneous cations in hybrid batteries, *Chemical*

*Communications*, 49(85), 9977-9979. <https://doi.org/10.1039/C3CC45895D>

4. Zheng F., Kotobuki M., Song Sh., Lai M. O., Li Lu. (2018) Review on solid electrolytes for all-solid-state lithium-ion batteries, *Journal of Power Sources*, vol. 389, pp. 198-213, <https://doi.org/10.1016/j.jpowsour.2018.04.022>.

5. Bucharsky E.C., Schell K.G., Hintennach A., Hoffmann M.J. (2015) Preparation and characterization of sol-gel derived high lithium ion conductive NZP-type ceramics Li<sub>1+x</sub>Al<sub>x</sub>Ti<sub>2-x</sub>(PO<sub>4</sub>)<sub>3</sub>, *Solid State Ionics*, vol. 274, pp.77-82, <https://doi.org/10.1016/j.ssi.2015.03.009>.

6. Sudreau F., Petit D., Boilot J.P.. (1989) Dimorphism, phase transitions, and transport properties in LiZr<sub>2</sub>(PO<sub>4</sub>)<sub>3</sub>, *Journal of Solid State Chemistry*, vol. 83, no.1, pp. 78-90, [https://doi.org/10.1016/0022-4596\(89\)90056-X](https://doi.org/10.1016/0022-4596(89)90056-X).

7. Jie Fu. (1997) Superionic conductivity of glass-ceramics in the system Li<sub>2</sub>O- Al<sub>2</sub>O<sub>3</sub>-TiO<sub>2</sub>-P<sub>2</sub>O<sub>5</sub>, *Solid State Ionics*, vol. 96, no. 3-4, pp. 195-200, [https://doi.org/10.1016/S0167-2738\(97\)00018-0](https://doi.org/10.1016/S0167-2738(97)00018-0).

8. Hallopeau L., Bregiroux D., Rousse G., Portehault D., Stevens P., Toussaint G., Laberty-Robert Ch. (2018) Microwave-assisted reactive sintering and lithium ion conductivity of Li<sub>1.3</sub>Al<sub>0.3</sub>Ti<sub>1.7</sub>(PO<sub>4</sub>)<sub>3</sub> solid electrolyte, *Journal of Power Sources*, vol. 378, pp. 48-52, <https://doi.org/10.1016/j.jpowsour.2017.12.021>.

9. Kwatek K., Nowiński J.L. (2017) Electrical properties of LiTi<sub>2</sub>(PO<sub>4</sub>)<sub>3</sub> and Li<sub>1.3</sub>Al<sub>0.3</sub>Ti<sub>1.7</sub>(PO<sub>4</sub>)<sub>3</sub> solid electrolytes containing ionic liquid, *Solid State Ionics*, vol. 302, pp. 54-60, <https://doi.org/10.1016/j.ssi.2016.11.020>.

10. Ma Q., Xu Q., Tsai Ch-L., Tietz F., Guillon O. (2016) A Novel Sol-Gel Method for Large-Scale Production of Nanopowders: Preparation of Li<sub>1.5</sub>Al<sub>0.5</sub>Ti<sub>1.5</sub>(PO<sub>4</sub>)<sub>3</sub> as an Example, *J. Am.*

Ceram. Soc. vol. 99, no. 2, pp. 410-414, <https://doi.org/10.1111/jace.13997>

11. Huang L., Wen Z., Wu M., Wu X., Liu Y., Wang X. J. (2011). Electrochemical properties of  $\text{Li}_{1.4}\text{Al}_{0.4}\text{Ti}_{1.6}(\text{PO}_4)_3$  synthesized by a co-precipitation method, *J. Power Sources*, vol. 196, pp. 6943–6946, <https://doi.org/10.1016/j.jpowsour.2020.11.140>

12. Tolganbek N., Mentbayeva A., Uzakbaiuly B., Kanamura K., Bakenov Zh. (2020)  $\text{Li}_{1+x}\text{Al}_x\text{Ti}_{2-x}(\text{PO}_4)_3$ , NASICON-type solid electrolyte fabrication with different methods, *Materials Today: Proceedings*, vol. 25, pp. 97-100, <https://doi.org/10.1016/j.matpr.2019.12.279>

13. Tolganbek Nurbol, Serikkazyeva Assel, Kalybekkyzy Sandugash, Sarsembina Madina, Kanamura Kiyoshi, Bakenov Zhumabay,

Mentbayeva Almagul. (2022) Interface modification of NASICON-type Li-ion conducting ceramic electrolytes: a critical evaluation, *Materials Advances*, vol. 3, pp. 3055-3069, 10.1039/D1MA01239H

14. Tianyu Zhao, Qixin Gai, Xiaoyan Deng, Junwei Ma, Hongtao Gao. (2023) A new type of LATP doped PVDF-HFP based electrolyte membrane with flame retardancy and long cycle stability for solid state batteries, *Journal of Energy Storage*, vol 73, <https://doi.org/10.1016/j.est.2023.108576>

15. Yen P., Lee M., Gregory D., Liu W. (2020) Optimization of sintering process on  $\text{Li}_{1+\text{Al}}\text{Ti}_2(\text{PO}_4)_3$  solid electrolytes for all-solid-state lithium-ion batteries, *Ceramics International*, vol. 46, pp. 20529–20536, <https://doi.org/10.1016/j.ceramint.2020.05.162>